

Near-Threshold Relaxation Dynamics of a Quantum Dot Laser

Cheng Wang^{a,b*}, Jacky Even^a and Frédéric Grillot^b

^aUniversité Européenne de Bretagne, INSA, CNRS FOTON, 20 avenue des buttes de Coesmes, 35708 Rennes Cedex 7, France

^bTelecom Paristech, Ecole Nationale Supérieure des Télécommunications, CNRS LTCI, 46 rue Barrault, 75013 Paris, France

ABSTRACT

The near-threshold dynamics of a QD and a commercial QW laser are investigated both experimentally and theoretically. Below threshold, the resonance frequency and damping factor of the QD laser exhibit a different behaviour as compared to the QW counterpart. In the near-threshold regime, the intra-dot carrier relaxation is predicted from an empirical pair-states model to have a strong impact on the QD laser's modulation dynamics. The widespread of experimental values for the damping factor reported in the literature for QD lasers is a further indication that this empirical approach is pushed to the limits in this situation. More accurate microscopic modelling should rely on a separation of electron and hole dynamics.

Keywords: semiconductor laser, quantum dot, modulation dynamics

1. INTRODUCTION

The quantum dot (QD) laser has been considered as a promising semiconductor laser source because of the three-dimensional quantum confinement of carriers [1]. In contrast to their quantum well (QW) counterpart, QD lasers provide many interesting features including lower threshold current density, higher temperature stability, reduced frequency chirp as well as a better resistance against parasitic optical reflections [2]. On the other hand, various studies have pointed out that the modulation characteristics of QD lasers are limited due to the low differential gain, the large gain compression factor as well as the complex carrier dynamics [3], [4]. Indeed, in the theoretical modeling of QD laser dynamics, many efforts have been devoted to take into account the intrinsic carrier dynamics of the nanostructure materials [5]-[10]. It is now well established that the slow carrier capture process from the carrier reservoir (identified as wetting layer in this work) into the QD is a limiting factor to the modulation bandwidth [11]. In this letter, the modulation dynamics of a QD laser is investigated close to the laser threshold. The same experimental set-up is used for a conventional quantum well (QW) device. Noteworthy, when reducing the bias current slightly below the threshold, the resonance frequency of the QD laser re-increases. From a theoretical analysis based on pair-states rate equation model, it is shown that the carrier relaxation process has a significant impact on the damping factor of the QD laser. The damping factor offset value is found to be almost inversely proportional to the carrier relaxation time, and also sensitive to the Pauli blocking factor of the excited state (ES). Finally this paper also points out the limitations of the pair states model in the context of the near-threshold dynamics of a QD laser.

2. EXPERIMENTAL OBSERVATIONS

In order to investigate the near-threshold dynamical behavior of QD lasers, the small-signal modulation response of a QD Fabry Perot laser device was experimentally studied. The QD structure was grown by the gas source molecular beam epitaxy on a 2° misoriented (100) n-doped InP substrate [12]. The active layer consists of 6 stack layers of InAs dots, which are embedded in an InGaAsP quaternary alloy. The structure was fabricated into 4- μm wide ridge waveguide, and finally the device was cleaved into a 830- μm long cavity. The laser's optical spectrum peaks around 1634.5 nm at threshold for room temperature operation. Detailed growth and basic properties of the QD laser have been described elsewhere [12], [13].

* cheng.wang@insa-rennes.fr; phone +33 223238464;

Figure 1 illustrates the experimental setup for studying the direct amplitude modulation dynamics of the QD laser. A DC bias current combined with a radio frequency (RF) modulation was applied to the laser device using a high-speed bias tee. The RF signal was generated from one port (port 1) of a vector network analyzer (VNA, Agilent Technologies, E5071C). The laser power was monitored by a power meter through the 10% branch of a 90/10 fiber splitter. 90% of the laser output was converted to RF signal by a high-speed photodiode, and then provided to the other port (port 2) of the VNA, where the amplitude response of the laser was recorded. The laser chip is mounted on a heat sink, and the operation temperature is maintained at 293 K by a thermoelectric controller (TEC). Prior to the measurement, a full two-port calibration was performed on the VNA to eliminate the parasitic and RF losses in the microwave cables and probes. As a comparison, a commercial QW laser was also studied in the same experimental setup. The resonance frequency and the damping factor at different bias current are extracted using the frequency response subtraction technique [14]. Before studying the near-threshold modulation dynamics of the QD and QW laser devices, it is necessary to clarify the definition of the laser's threshold in the measurements. Fig. 2 depicts the coupled output power versus the pump current (known as L-I curve) in the double-log scale. The lasing threshold locates in the steepest part of the S-like curve [15]. With the help of the optical spectrum analyzer, the threshold current is defined as the point at which several sharp longitudinal modes emerge from the smooth optical spectra. Thus, at room temperature, the threshold currents are measured to be 63.5 mA for the QD laser and 22 mA for the QW laser.

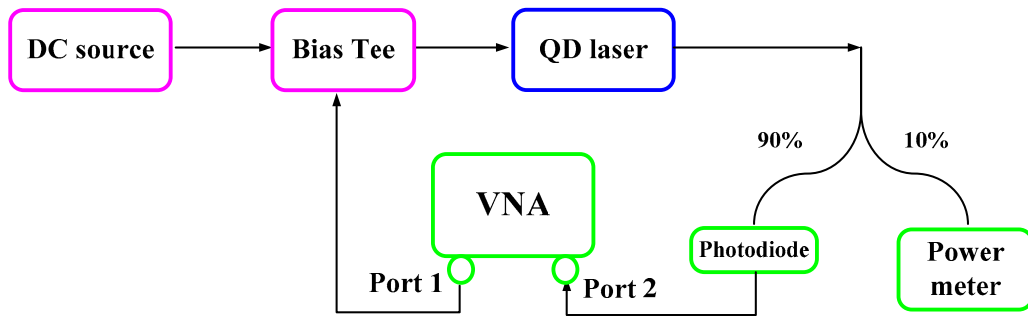


Figure 1. Schematic of the laser device characterization experimental setup.

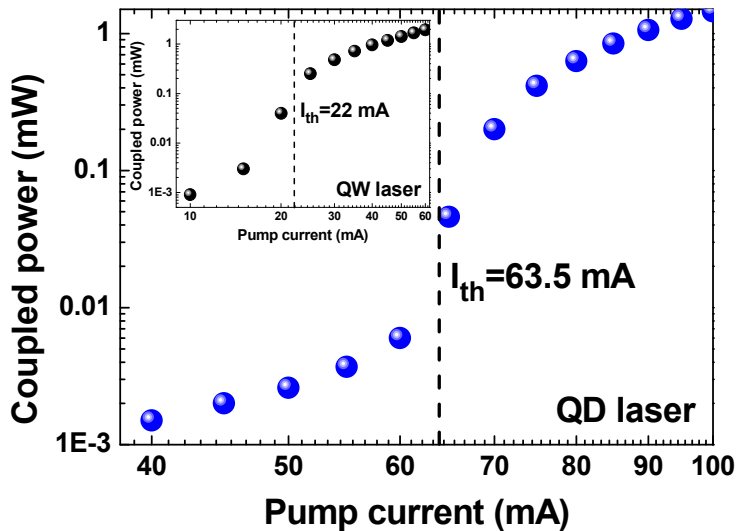


Figure 2. Room temperature measured L-I curves in log-log scale for the QD laser and the QW laser (inset). The threshold currents are 63.5 mA and 22 mA, respectively, which are identified together with the optical spectrum.

When reducing the bias current slightly below the threshold, the resonance frequency (f_R) of the QW laser keeps decreasing and approaches a limiting value (inset of Fig. 3) rather than zero. This phenomenon has already been observed in [16], and the resonance behavior is attributed to the noise fluctuations in the photon field, which arises from the spontaneous emission as well as to the optical absorption and scattering. In contrast, for the case of the QD laser in Fig. 3, the resonance frequency re-increases when the laser is operated close to the lasing threshold. The simulation data (red stars) obtained from a standard pair-states model (vide infra) are qualitatively in good agreement with the experimental result (blue spheres). This specific behaviour is explained by the Pauli blocking for the ES to the ground state (GS) relaxation, which increases with a reduced bias current.

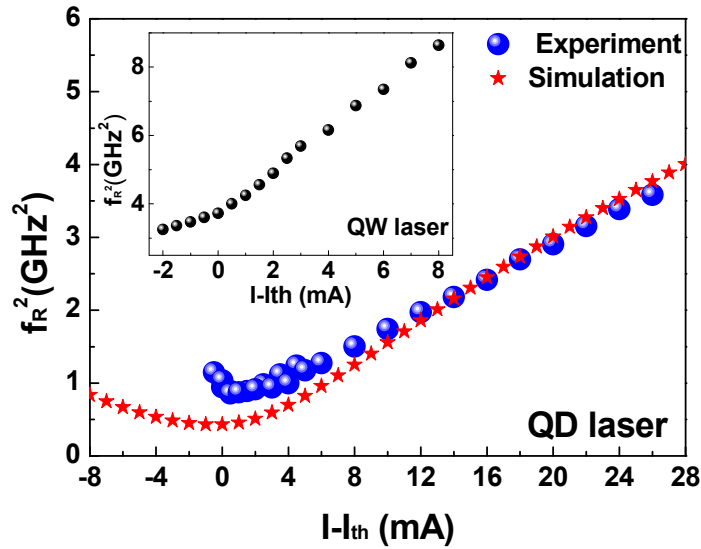


Figure 3. Square of resonance frequency versus the normalized bias current $I-I_{th}$. Spheres are the experimental results and stars denote the simulation data. Inset is the case of the commercial QW laser for comparison.

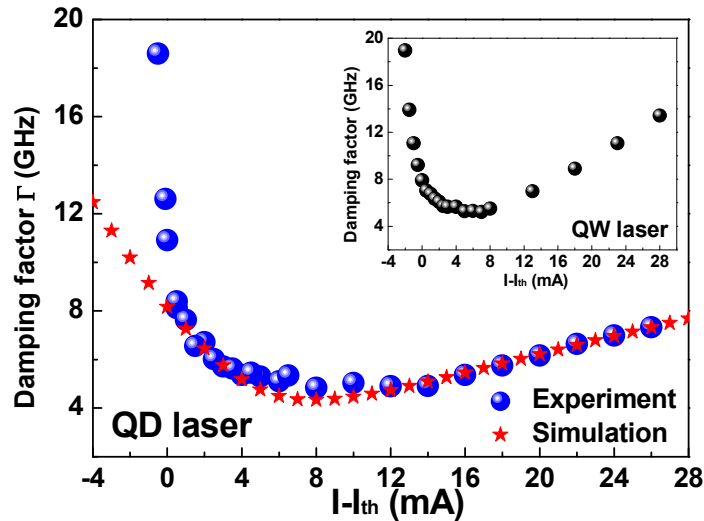


Figure 4. Damping factor of the QD laser versus the normalized current $I-I_{th}$. In the simulation, the key parameters for fitting the near-threshold experimental result are $\tau_{GS}^{ES} = 45$ ps, $N_B = 6 \times 10^{10}/\text{cm}^2$ and $\beta_p = 10^{-3}$. Inset is the case of the QW laser.

For the damping factor (Γ) shown in Fig. 4, the QD laser exhibits a similar near-threshold behaviour as the QW laser (inset). The simulation also matches quite well with the experimental data. The deviation from linearity close to threshold is mainly due to the spontaneous emission [17], and on the other hand to the variation of the Pauli blocking effect of the ES. When plotting Γ versus f_R^2 for the QD laser, an offset value of $\Gamma_0=2.4$ GHz (associated with a K-factor of 1.7 ns) is obtained by linear curve-fitting, which is slightly larger than that of the QW laser ($\Gamma_0=2.0$ GHz). The modulation dynamics of semiconductor lasers is characterized by the resonance frequency f_R and the damping factor Γ , which are phenomenologically linked by the so-called K-factor as $\Gamma = Kf_R^2 + \Gamma_0$ with Γ_0 the damping factor offset at threshold. The $1/\Gamma_0$ constant usually defines the effective carrier lifetime of the device. Table I summarizes typical experimental Γ_0 and K-factor values reported in the literature for QD lasers [3], [4], [18]-[21]. It is found that Γ_0 spreads out over a wide range from 1.7 GHz up to 17.0 GHz, which is generally larger than that of QW lasers (1-2 GHz) [22]. The values found experimentally in this work are in the range of those typically found for QD lasers.

Table I. K-factor and damping factor offset values of QD lasers reported in the literature

Ref.	Laser type	K-factor	Γ_0
18	InGaAs/GaAs (FP)	1.20 ns	17.0 GHz
4	InAs/InGaAs (DFB)	1.02 ns	9.9 GHz
19	InAs/GaAs (FP)	1.51 ns	9.0 GHz
20	InAs/GaAs (FP)	1.44 ns	7.5 GHz
3	InAs/InP(311)B (FP)	0.63 ns	3.0 GHz
21	InAs/GaAs (DFB)	0.23 ns	1.7 GHz
This work	InAs/InP(100) (FP)	1.70 ns	2.4 GHz

3. THEORETICAL STUDIES

Semi-empirical modeling of the dynamical properties of QD devices often relies on a slightly extended version of the pair-states rate equation model for bulk and QW semiconductors [22]. Despite its conceptual simplicity, it yields in various cases a good description of QD laser dynamical properties with a reasonable number of empirical parameters. The standard model used here holds under the assumption that the active region consists of only one QD ensemble, where QDs are interconnected within the wetting layer (WL) [5], [6], [23], [24]. The QD ensemble includes two pair states: a ground state (GS) and an excited state (ES). The QDs are assumed to be always neutrally charged, electrons and holes are treated as electron-hole pairs. Moreover, the electron and hole are expected to be found simultaneously in their mono-electronic ground states (GS pair state) or first excited states (ES pair state). A situation corresponding to one carrier in its GS and the other in an ES is typically disregarded to simplify the model. These microscopic configurations yield weak or forbidden radiative recombinations for typical QD geometries.

The QD laser system is described in the pair-states model by the following four coupled rate equations:

$$\frac{dN_{WL}}{dt} = \frac{I}{q} + \frac{N_{ES}}{\tau_{WL}^{ES}} - \frac{N_{WL}}{\tau_{ES}^{WL}} P_{ES} - \frac{N_{WL}}{\tau_{WL}^{spon}} \quad (1)$$

$$\frac{dN_{ES}}{dt} = \frac{N_{WL}}{\tau_{ES}^{WL}} P_{ES} + \frac{N_{GS}}{\tau_{ES}^{GS}} P_{ES} - \frac{N_{ES}}{\tau_{WL}^{ES}} - \frac{N_{ES}}{\tau_{GS}^{ES}} P_{GS} - \frac{N_{ES}}{\tau_{ES}^{spon}} \quad (2)$$

$$\frac{dN_{GS}}{dt} = \frac{N_{ES}}{\tau_{GS}^{ES}} P_{GS} - \frac{N_{GS}}{\tau_{ES}^{GS}} P_{ES} - \frac{N_{GS}}{\tau_{GS}^{spon}} - \Gamma_P g v_g S \quad (3)$$

$$\frac{dS}{dt} = \Gamma_P g v_g S - \frac{S}{\tau_P} + \beta_{SP} \frac{N_{GS}}{\tau_{GS}^{spon}} \quad (4)$$

where $N_{WL,ES,GS}$ are carrier numbers in WL, ES, GS, S the photon number of GS in the cavity, τ^{spont} the spontaneous emission time, β_{sp} the spontaneous emission factor, Γ_p the optical confinement factor, τ_p the photon lifetime and v_g the group velocity. The carrier transport processes in the barrier are not taken into account. Then carriers are supposed to be thermalized into the reservoir directly from the contact. Once in the WL, the carriers are firstly captured into the ES of the dots within a time τ_{ES}^{WL} before relaxing into the GS within a time τ_{GS}^{ES} . $P_{GS,ES}$ are the Pauli blocking factors of the GS and the ES, respectively. The QD laser parameters used in the simulation are listed in Table II.

Table II. The QD material parameters and the laser parameters

QD material parameters		Laser parameters	
WL energy:	$E_{WL}=0.97$ eV	Active region length:	$L=0.11$ cm
ES energy:	$E_{ES}=0.87$ eV	Active region width:	$W=3 \times 10^{-4}$ cm
GS energy:	$E_{GS}=0.82$ eV	Number of QD layers:	$N=5$
Capture time from WL to ES:	$\tau_{ES}^{WL}=25.1$ ps	QD density:	$N_D=5 \times 10^{10}$ cm ⁻²
Relaxation time from ES to GS:	$\tau_{GS}^{ES}=11.6$ ps	Optical confinement factor:	$\Gamma_p=0.06$
Spontaneous time of WL and ES:	$\tau_{WL}^{spont} = \tau_{ES}^{spont} = 500$ ps	Spontaneous emission factor:	$\beta_{sp}=1 \times 10^{-4}$
Spontaneous time of GS:	$\tau_{GS}^{spont}=1200$ ps	Internal modal loss:	$\alpha_i=6$ cm ⁻¹
Refractive index:	$n_r=3.27$	Mirror reflectivity:	$R_1=R_2=0.3$

In a previous work, we analytically derived the modulation transfer function of the QD laser [23]. Particularly, the expressions of resonance frequency and damping factor were improved as follows:

$$\omega_R^2 = \frac{v_g a_{GS} S^D}{\tau_p} + \left(\Gamma_p v_g a_{GS}^p S^D + \frac{\Gamma_p \beta_{SP} N_{GS}^D}{\tau_{GS}^{spont} S^D} \right) \left(\frac{P_{ES}}{\tau_{ES}^{GS}} + \frac{1 - \beta_{SP}}{\tau_{GS}^{spont}} \right) + \frac{\beta_{SP}}{\tau_{GS}^{spont} \tau_p} \quad (5)$$

$$\Gamma = v_g a_{GS} S^D \left(1 + \frac{\Gamma_p a_{GS}^p}{a_{GS}} \right) + \frac{\Gamma_p \beta_{SP} N_{GS}^D}{\tau_{GS}^{spont} S^D} + \Gamma_0 \quad (6)$$

with the damping factor offset:

$$\Gamma_0 = \frac{P_{ES}}{\tau_{ES}^{GS}} + \frac{1}{\tau_{GS}^{spont}} \quad (7)$$

where a_{GS} is the differential gain, N_{GS}^D, S^D respectively are the carrier and photon densities. It is important to note that, in contrast to the case of QW lasers, an additional term P_{ES} / τ_{ES}^{GS} appears in equations (5)-(7). Thus, both the Pauli blocking factor of the ES and the intra-dot carrier escape process potentially have significant impact on the near-threshold dynamical behaviours. Close to the lasing threshold, the photon number in the cavity is small and can be neglected. Equations (5) and (6) are then re-expressed as:

$$\omega_R^2 \approx \frac{\Gamma_p \beta_{SP} N_{GS}^D}{\tau_{GS}^{spont} S^D} \left(\frac{P_{ES}}{\tau_{ES}^{GS}} + \frac{1 - \beta_{SP}}{\tau_{GS}^{spont}} \right) + \frac{\beta_{SP}}{\tau_{GS}^{spont} \tau_p} \quad (8)$$

$$\Gamma \approx \frac{\Gamma_p \beta_{SP} N_{GS}^D}{\tau_{GS}^{spon} S^D} + \Gamma_0 \quad (9)$$

These expressions show that the spontaneous emission process plays an important role in the near-threshold relaxation dynamics for both QW and QD lasers. The spontaneous emission might lead to a finite resonance and damping even slightly below threshold. However, it is important to realize that the β_{SP} term is usually ignored for the well above-threshold analysis [24], which is no longer valid for the near-threshold condition. For QD lasers the additional P_{ES} / τ_{ES}^{GS} term drives the near-threshold relaxation behavior as well. For the damping factor Γ , it is well known that in QW lasers the offset value Γ_0 is directly influenced by the microscopic spontaneous emission. In contrast, in QD lasers the Γ_0 value does not only depend on the spontaneous emission but also on the intra-dot scattering and thus the ES Pauli blocking factor P_{ES} associated with the intra-dot carrier escape rate $1 / \tau_{ES}^{GS}$ (equation 7). Indeed, Fig. 5 shows that the damping factor offset (black spheres) is almost inversely proportional to the carrier relaxation time. This result gives insight to understand such a wide spread Γ_0 of QD lasers as shown in Table I. In addition, a slow carrier relaxation rate also leads to a slight reduction of the Pauli blocking factor of the ES (blue squares). Fig. 6 shows the damping factor and the resonance frequency extracted from the modulation responses. When increasing the carrier relaxation time from 5.0 ps to 100 ps, the resonance frequency (blue squares) is reduced by about 1.5 GHz. The same trend is obtained for the variation depicted as a function of the carrier capture time (Inset). The calculated damping factor value (black spheres) decreases with increasing carrier relaxation time, from 41 GHz (for $\tau_{GS}^{ES}=5.0$ ps) down to 3.0 GHz (for $\tau_{GS}^{ES}=100$ ps). In contrast, the resonance frequency changed by the carrier capture process (inset) is only about 2.5 GHz. The impact of the relaxation process on the damping factor is attributed to the carrier escape process from the GS to the ES as expressed in equation (7).

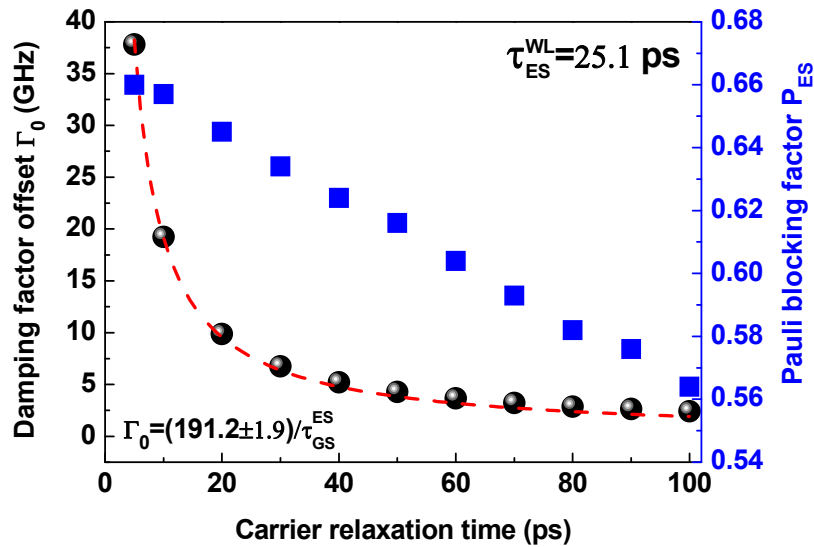


Figure 5. The damping factor offset Γ_0 (black spheres) as a function of the carrier relaxation time τ_{GS}^{ES} . The blue squares denote the corresponding variation of the Pauli blocking factor of the ES at threshold. The dashed line is the least squares fitting of Γ_0 versus τ_{GS}^{ES} .

Generally, two microscopic mechanisms are responsible for the carrier relaxation process. One is the phonon-assisted relaxation when a hot carrier relaxes to the GS with emission of one or few phonons, which dominates at low excitation densities [25]. Another one is the faster Auger process, which depends nonlinearly on the carrier density [26]-[28]. The

Auger scattering rate can change appreciably, the reported relaxation times of QD lasers at room temperature are typically in the 1.0-100 ps range [29], [30]. The strong dependence of the near-threshold QD laser dynamics on the carrier relaxation probably pushes the pair states model to the limits of relevancy. The widespread of reported K-factor and damping factor offset values of QD lasers (table I) can be hardly interpreted without relying on a more detailed analysis. Indeed, these parameters can be considered as fingerprints of the material system, QD growth and technological design of such devices. QD lasers can be more accurately described utilizing a semi-classical approach separating electrons and holes dynamics within the semiconductor-Bloch framework [31]. Such an approach can be used to describe quantum-coherent effects by taking into account the microscopic polarization of the optical transitions within an inhomogeneously broadened QD medium. It is possible to link such a microscopic QD laser model to the empirical pair-states one through the adiabatic elimination of the microscopic polarization and the introduction of some phenomenological terms [32]. Auger relaxation processes have been analyzed separately for electrons and holes in InAs/InP (100) based QD structures similar to the ones used in the present work [33]. Similar relaxation times are predicted, but the complete hole dynamics is probably severely impacted by the large number of closely spaced confined states in the QD by contrast to the electrons [34]. It has been recently shown that the regime of strongly damped relaxation oscillations such as the one occurring near-threshold is highly sensitive to the details of electrons and holes dynamics and different confinement potentials [35]. This leads to different dynamic scenarios for the QD laser depending on whether or not electrons and holes can be considered as having similar dynamics. These configurations can not be captured by the simplified pair-states model.

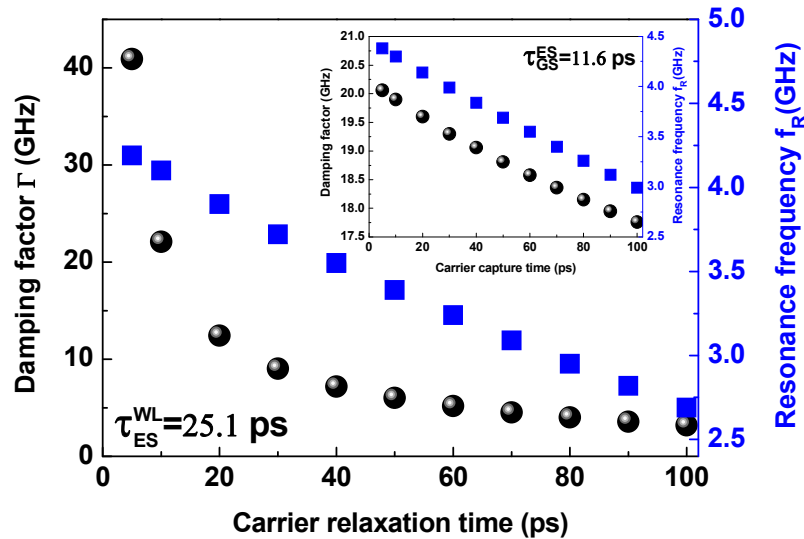


Figure 6. Damping factor (black spheres) and resonance frequency (blue squares) for various carrier relaxation times of the corresponding modulation responses shown in Fig.1. Inset is the case for various carrier capture times. The QD laser is biased above threshold at $I=1.5 \times I_{th}$.

4. CONCLUSION

In summary, the near-threshold dynamics of a QD laser has been investigated both experimentally and theoretically. The intra-dot carrier relaxation driven by many-body processes is predicted to have a strong impact on the modulation dynamics of QD lasers in the below-threshold regime. The widespread of experimental values reported in the literature for QD lasers is a further indication that the approach based on a simplified pair-states model is pushed to the limits in this situation. More accurate modeling should rely on a separation of electron and hole dynamics.

ACKNOWLEDGMENTS

The authors would like to thank B. Lingnau, Dr. K. Lüdge and Pr. E. Schöll from TU Berlin for helpful discussions. Dr. F. Grillot is supported by the European Office of Aerospace Research and Development (EOARD) under grant number FA8655-12-1-2093 and by Deutscher Akademischer Austauschdienst (DAAD). C. Wang's work is supported by China Scholarship Council. Professor J. Even is supported by DAAD.

REFERENCES

- [1] Arakawa, Y., and Sakaki, H., "Multidimensional quantum well laser and temperature dependence of its threshold current," *Appl. Phys. Lett.* 40(11), 939-941 (1982).
- [2] Bimberg, D., Grundmann, M., and Ledentsov, N. N., [Quantum Dot Heterostructures], New York: Wiley, (1999).
- [3] Martinez, A. *et al.*, "Dynamic properties of InAs/InP (311B) quantum dot Fabry-Perot lasers emitting at 1.52- μm ," *Appl. Phys. Lett.* 93(2), 021101 (2008).
- [4] Zhukov, A. E. *et al.*, "Gain compression and its dependence on output power in quantum dot lasers," *J. Appl. Phys.* 113(23), 233103 (2013).
- [5] Veselinov, K., Grillot, F., Cornet, C., Even, J., Bekiarski, A., Gioannini, M., and Loualiche, S., "Analysis of the double laser emission occurring in 1.55- μm InAs-InP (113)B quantum-dot lasers," *IEEE J. Quantum. Electron.* 43(9), 810-816 (2007).
- [6] Grillot, F., Veselinov, K., Gioannini, M., Montrosset, I., Even, J., Piron, R., Homeyer, E., Loualiche, S., "Spectral analysis of 1.55 μm InAs-InP(113)B quantum-dot lasers based on a multipopulation rate equation model," *IEEE J. Quantum. Electron.* 45(7), 872-878 (2009).
- [7] Gioannini, M., Sevega, A., and Montrosset, I., "Simulations of differential gain and linewidth enhancement factor of quantum dot semiconductor lasers," *Optic. and Quantum Electron.* 38, 381-394 (2006).
- [8] Erneux, T., Viktorov, E. A., and Mandel, P., "Time scales and relaxation dynamics in quantum-dot lasers," *Phys. Review A* 76(2), 023819 (2007).
- [9] Markus, A., Chen, J. X., Lafaye, O. G., Provost, J. G., Paranthoen, C., and Foire, A., "Impact of intraband relaxation on the performance of a quantum-dot laser," *IEEE J. sel. Top. Quantum. Electron.* 9(5), 1308-1314 (2003).
- [10] Sugawara, M., Mukai, K., Nakata, Y., and Ishikawa, H., "Effect of homogeneous broadening of optical gain on lasing spectra in self-assembled $\text{In}_x\text{Ga}_{1-x}/\text{GaAs}$ quantum dot lasers," *Phys. Review B* 61(11), 7595-7603 (2000).
- [11] Lelarge, F. *et al.*, "Recent advances on InAs/InP quantum dash based semiconductor lasers and optical amplifiers operating at 1.55 μm ," *IEEE J. sel. Top. Quantum. Electron.* 13(1), 111-124 (2007).
- [12] Wang, C., Grillot, F., Lin, F. Y., Aldaya, I., Batte, T., Gosset, C., Decerle, E., and Even, J., "Nondegenerate four-wave mixing in a dual-mode injection-locked InAs/InP(100) nanostructure laser," *IEEE Photon. Journal* 6(1), 1500408 (2014).
- [13] Elias, G. *et al.*, "Achievement of high density InAs/GaInAsP quantum dots on misoriented InP(001) substrates emitting at 1.55 μm ," *Jpn. J. of Appl. Phys.* 48(7), 070204 (2009).
- [14] Morton, P. A., Tanbun-Ek, T., Logan, R. A., Sergeant, A. M., Sciortino, R. F., and Coblenz, D. L., "Frequency response subtraction for simple measurement of intrinsic laser dynamic properties," *IEEE Phonon. Technol. Lett.* 4(2), 133-136 (1992).
- [15] Ning, C. Z., "What is laser threshold," *IEEE J. sel. Top. Quantum. Electron.* 19(4), 1503604 (2013).
- [16] Paoli, T. L., "Near-threshold behaviour of the intrinsic resonant frequency in a semiconductor laser," *IEEE J. Quantum. Electron.* QE-15(8), 807-812 (1979).
- [17] Su, C. B., Eom, J., William, C., Rideout, C., Lange, H., Kim, C. B., Lauer, R. B., and Lacourse, J. S., "Characterization of the dynamics of semiconductor lasers using optical modulation," *IEEE J. Quantum Electron.* 28(1), 118-127 (1992).
- [18] Kuntz, M., [Modulated InGaAs/GaAs Quantum Dot Lasers], Ph. D thesis, Berlin, (2006).
- [19] Naderi, N. A., [External Control of Semiconductor Nanostructure Lasers], Ph. D thesis, New Mexico, (2011).
- [20] Pochet, M. C., [Characterization of the Dynamics of Optically-Injected Nanostructure Lasers], Ph. D thesis, New Mexico, (2010).
- [21] Su, H., [Dynamic Properties of Quantum Dot Distributed Feedback Lasers], Ph. D thesis, New Mexico, (2004).
- [22] Coldren, L. A., and Corzine, S. W., [Diode Lasers and Photonic Integrated Circuits], New York: Wiley, (1995).

- [23] Wang, C., Grillot, F., and Even, J., "Impacts of wetting layer and excited state on the modulation response of quantum-dot lasers," *IEEE J. Quantum. Electron.* 48(9), 1144-1150 (2012).
- [24] Lüdge, K., Schöll, E., Viktorov, E., and Erneux, T., "Analytical approach to modulation properties of quantum dot lasers," *J. Appl. Phys.* 109(10), 103112 (2011).
- [25] Miska, P., Even, J., Dehaese, O., and Marie, X., "Carrier relaxation dynamics in InAs/InP quantum dots," *Appl. Phys. Lett.* 92(19), 191103 (2008).
- [26] Ohnesorge, B., Albrecht, M., Oshinowo, J., Forchel, A., and Arakawa, Y., "Rapid carrier relaxation in self-assembled $\text{In}_x\text{Ga}_{1-x}\text{As}/\text{GaAs}$ quantum dots," *Phys. Review B* 54(16), 11532-11538 (1996).
- [27] Majer, N., Lüdge, K., and Schöll, E., "Cascading enables ultrafast gain recovery dynamics of quantum dot semiconductor optical amplifiers," *Phys. Review B* 82(23), 235301 (2010).
- [28] Ignatiev, I. V., and Kozin, I. E., "Carrier relaxation dynamics in InP quantum dots studied by artificial control of nonradiative losses," *Phys. Review B* 61(23), 15633-15636 (2000).
- [29] Heitz, R., Kalburge, A., Xie, Q., Grundmann, M., Chen, P., Hoffmann, A., and Bimberg, D., "Excited states and energy relaxation in stacked InAs/GaAs quantum dots," *Phys. Review B* 57(15), 9050-9060 (1998).
- [30] Foire, A., Borri, P., Lanbein, W., Hvam, J. M., Oesterle, U., Houdre, R., Stanley, R. P., and Illegems, M., "Time-resolved optical characterization of InAs/InGaAs quantum dots emitting at 1.3 μm ," *Appl. Phys. Lett.* 80(23), 3430 (2000).
- [31] Chow, W. W., Sargent, M., Koch, S. W., [Semiconductor Laser Physics], Springer-Verlag, (1994).
- [32] Lingnau, B., Chow, W. W., Schöll, E., and Lüdge, K., "Feedback and injection locking instabilities in quantum-dot lasers: a microscopically based bifurcation analysis," *New J. Phys.*, 15(9), 093031 (2013).
- [33] Even, J., Pedesseau, L., Dore F., and Boyer-Richard, S., "InAs QDs on InP: polarization insensitive SOA and non-radiative Auger processes," *Opt. Quant. Electron.* 40, 1233-1238 (2008).
- [34] Gioannini, M., "Ground-state power quenching in two-state lasing quantum dot lasers," *J. Appl. Phys.* 111(4), 043108 (2012).
- [35] Lingnau, B., Lüdge, K., Chow, W. W., and Schöll, E., "Influencing modulation properties of quantum-dot semiconductor lasers by carrier lifetime engineering," *Appl. Phys. Lett.* 101(13), 131107 (2012).